THE JOURNAL OF PHYSICAL CHEMISTRY LETTERS
A JOURNAL OF THE AMERICAN CHEMICAL SOCIETY

pubs.acs.org/JPCL Letter

Pressure-Induced Hydrogen Transfer in 2-Butyne via a Double CH···π Aromatic Transition State

Peijie Zhang,[▽] Xingyu Tang,[▽] Chunfang Zhang, Dexiang Gao, Xuan Wang, Yajie Wang, Wenhan Guo, Ruqiang Zou, Yehua Han, Xiaohuan Lin, Xiao Dong, Kuo Li, Haiyan Zheng,* and Ho-kwang Mao

Cite This: *J. Phys. Chem. Lett.* 2022, 13, 4170–4175 Read Online

ACCESS | Metrics & More | Article Recommendations | Supporting Information

ABSTRACT: Hydrogen transfer (H-transfer) is an important elementary reaction in chemistry and bioscience. It is often facilitated by the hydrogen bonds between the H-donor and acceptor. Here, at room temperature and high pressure, we found that solid 2-butyne experienced a concerted two-in−two-out intermolecular CH···π H-transfer, which initiated the subsequent polymerization. Such double H-transfer goes through an aromatic Hückel six-membered ring intermediate state via intermolecular CH···π interactions enhanced by external pressure. Our work shows that H-transfer can occur via the CH···π route in appropriate conformations under high pressure, which gives important insights into the H-transfer in solid-state hydrocarbons.

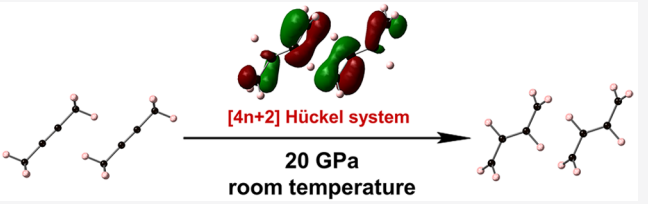

Hydrogen is the most abundant element in the universe, and hydrogen transfer (H-transfer) under high pressure is of great importance to petroleum science, geoscience, planetary science, chemistry, and bioscience. It is the key step in the C−H circulation inside the earth, the reaction of organics and inorganics in giant planets,[1−3] and the synthesis of high-temperature superconductors.[4] Typical H-transfer usually occurs via a hydrogen bond (H-bond), which can be tuned in very small steps but on very large energy scales under high pressure, hence changing the kinetics and even the thermodynamics of the H-transfer. For example, in ice the classical O···HO ↔ OH···O double-well H-bond becomes symmetric at about 100 GPa.[5,6] The moderate N−H···N H-bond in solid NH_3 was predicted to lead to H-transfer and form NH_4^+ and NH_2^- under high pressure.[7] Even a much weaker hydrogen bond, CH···N in solid CH_3CN, was reported to induce H-transfer from methyl to the N atom under high pressure.[8] Similarly, in the pressure-induced polymerization (PIP) of pyridine, the hydrogenation of nitrogen was also observed.[9−12] In enzymatic H-transfer reactions, pressure would decrease the reaction barrier and increase the catalytic rate, which is also related to the variation of the H-bond under high pressure.[13]

From the above discussion, it seems that the H-bond is a prerequisite for H-transfer. On the other hand, as a kind of weak interaction, the CH···π interaction is extensively present in aromatic, alkene, and alkyne compounds and has been widely investigated in supramolecular chemistry.[14−17] The CH···π interaction can be enhanced/modified upon compression, such as the shift in the CH···π-bonded sheets in the high-pressure phase transition of benzene.[18] Until now, there has been no report on the H-transfer from a saturated carbon to the unsaturated carbon of the arene or alkyne at room temperature without a catalyst, owing to the weak intermolecular interaction and the inertness of the C−H bond. In this work, we investigated the high-pressure chemical transformations of solid 2-butyne (C_4H_6), which has extensive intermolecular C−H···π interactions. We found that under high pressure the methyl hydrogen is transferred to the ethynyl group of the adjacent molecule via the C−H···π path, which leads to the isomerization of 2-butyne and a new polymerization route instead of the direct addition of unsaturated bonds.[19−22] It is an intermolecular concerted H-transfer of 2-butyne via an aromatic Hückel six-membered ring intermediate state, resulting in the formation of more stable 1,3-butadiene. Such a H-transfer process is probably widely applied between other saturated and unsaturated hydrocarbons in the dense solid under high pressure.[23]

We measured in situ Raman and IR spectroscopy of 2-butyne at up to 32 GPa (Figure 1a,b, peak assignments in Table S1, more data in Figure S1). The liquid 2-butyne solidified at 0.9 GPa into phase I ($P4_2/mnm$, molecules aligned parallel inside the layers with the orientation perpendicular to that of adjacent layers) and transformed to phase II ($C2/m$, all molecules aligned parallel) at 1.7 GPa as reported.[24,25] Above 14.1 GPa, phase II was amorphized or reacted because all Raman peaks disappeared (Figure 1a). When recovered from 18.8 GPa, a colorless solid was obtained, and an intense Raman

Received: March 26, 2022
Accepted: April 29, 2022
Published: May 4, 2022

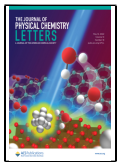

https://doi.org/10.1021/acs.jpclett.2c00877
J. Phys. Chem. Lett. 2022, 13, 4170−4175

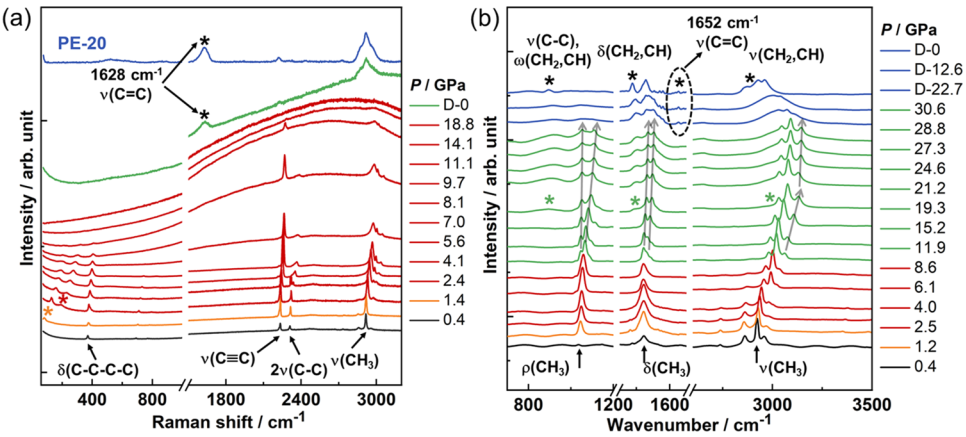

Figure 1. Selected Raman and IR spectra of 2-butyne under high pressure. (a) In situ Raman spectra from 0.4 to 18.8 GPa during compression and decompression (D-pressure) and Raman spectrum of the recovered PE-20 sample at ambient pressure. PE-20 stands for the sample recovered at 20 GPa by using the PE press. (b) In situ IR spectra of 2-butyne from 0.4 to 30.6 GPa during compression and decompression (D-pressure). D-0 stands for the sample recovered at ambient pressure. The gray arrows represent the splitting or enhancing of peaks related to methyl groups. The asterisks highlight the appearance of new peaks. More data are available in the Supporting Information.

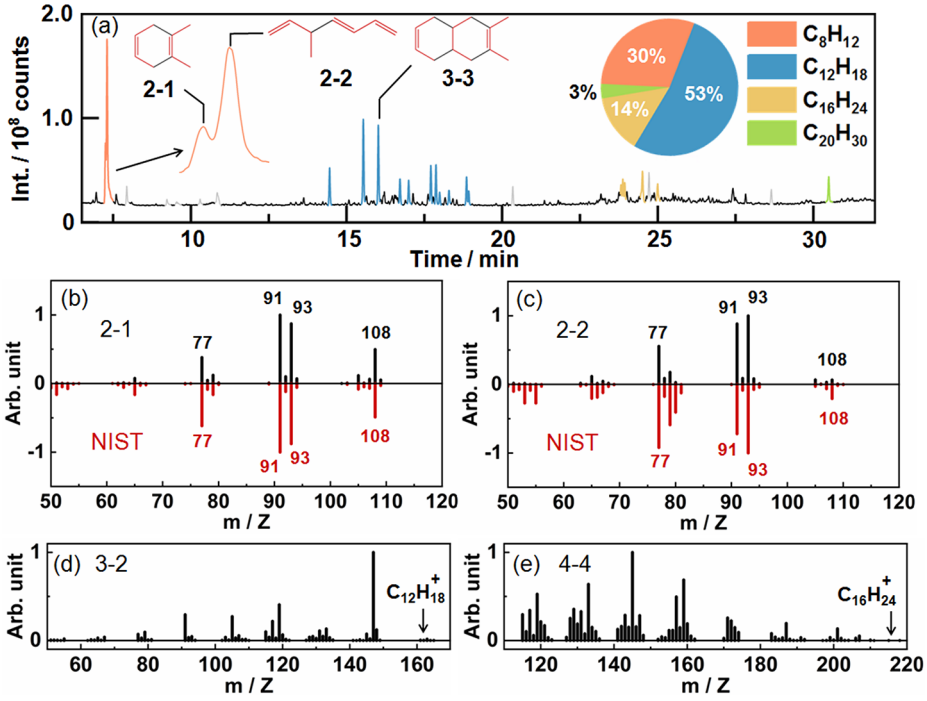

Figure 2. (a) Gas chromatography of the components extracted from the PE-20 sample by *n*-hexane, with the inset pie chart showing the contents of the components. Nineteen compounds with content higher than 1% were marked with matching colors according to the degree of polymerization. The black peaks represent those with content lower than 1%, and the peaks in gray stand for column bleeding. **2-1**, **2-2**, and **3-3** were identified by comparing the mass spectra (MS) data with the National Institute of Standards and Technology (NIST) database, and the C4 residual of the monomer is shown by a red line. The MS comparison with NIST spectra of (b) **2-1** and 1,2-dimethylcyclohexa-1,4-diene and (c) **2-2** and *trans*-5-methyl-1,3,6-heptatriene. MS data of (d) **3-2** (the most abundant trimer) and (e) **4-4** (the most abundant tetramer).

peak at 1628 cm^{-1} was observed, which was assigned to C═C stretching mode ν(C═C) (green line in Figure 1a). Likewise, the sample synthesized via a Paris-Edinburgh (PE) press at 20 GPa (referred to as PE-20) is also a colorless solid dominated by sp^2 carbon (blue line in Figure 1a).

An in situ IR investigation provides more information on the variation of methyl groups. At 11.9 GPa, the CH_3 rocking vibration $\rho(CH_3)$ and CH_3 deformation vibration $\delta(CH_3)$ at 1061 and 1443 cm^{-1}, respectively, started to split, and the C−H stretching at 3062 cm^{-1} was enhanced (Figure 1b; see Figure S2 for details). This is likely due to the conformational changes of methyl in the crystal. At 21.2 GPa, two distinct new bands appeared at 892 and 1402 cm^{-1} (Figure 1b). The former is in the region of C−C stretching vibration ν(C−C) and CH_2 or CH wagging vibration $\omega(CH_2, CH)$, and the latter is ascribed to new CH_2 or CH deformation vibrations $\delta(CH_2, CH)$.[26] In addition, a shoulder at 2975 cm^{-1} was observed on the low-frequency side of the CH_3 stretching $\nu(CH_3)$, which is assigned to the C−H stretching of CH_2 or CH, $\nu(CH_2, CH)$.[26] These features indicate that the methyl group of 2-butyne was transformed to a methylene ($-CH_2-$) or methyne group (R_3CH) during compression, with some hydrogen atoms

https://doi.org/10.1021/acs.jpclett.2c00877
J. Phys. Chem. Lett. 2022, 13, 4170−4175

leaving the methyl group. Upon decompression, a peak at 1652 cm^{-1} ascribed to ν(C═C) was observed (Figure 1b), suggesting that the subsequent reaction proceeding extensively in the decompression. These new peaks are maintained in the solid sample after recovery to ambient pressure (asterisk in Figure 1b), which shows the irreversible H-transfer and polymerization of 2-butyne, with sp C converting to sp^2 C and a part of CH_3 converting to CH_2 or CH. We can conclude that 2-butyne undergoes conformational transitions above 11.9 GPa, obvious H-transfer reactions above 21.2 GPa, and extensive polymerization during decompression.

To understand the H-transfer and the subsequent polymerization, we extracted the soluble molecules (oligomers) from the colorless PE-20 sample. High-resolution gas chromatography mass spectrometry (HRGC−MS) with an electron ionization (EI) source and chemical ionization (CI) was employed to identify these oligomers, and the results are shown in Figure 2 and Figures S3 and S4, respectively. Nineteen compounds with content greater than 1% were detected, including 2 dimers (C_8H_{12}), 11 trimers ($C_{12}H_{18}$), 5 tetramers ($C_{16}H_{24}$), and 1 pentamer ($C_{20}H_{30}$) as shown in Figure 2a and Table S2. Polymers with a degree of polymeization n from 6 to 14 were also identified with a matrix-assisted laser desorption/ionization time-of-flight mass spectrometry (MALDI-TOF−MS) experiment on the insoluble solid (Figure S5). All of these molecules have a composition of $(C_4H_6)_n$, showing no hydrogen atoms or carbon fragments such as H_2, CH_4, or C_2H_4 eliminated or added. This is very different from the products of free radical polymerizations, which usually have a C/H ratio slightly different from that of reactants because the produced intermediates often need to gain or lose a radical (such as H·) to terminate the chain reaction and hence change the oxidation state of carbon. For example, C_4H_6, C_4H_2, and C_6H_8 are detected in the hydrolysis product of the polymerized NaC_2H sample recovered from high pressure, whereas the product would be $(C_2H_2)_n$ if no H· is gained or lost.[20] Considering the CH_2 or CH observed in the IR data, we conclude that the PIP of 2-butyne does not result from polymerization across neighboring triple bonds but rather other reaction routes, including H-transfer, that need to be identified.

For the structure of oligomers, the two dimers (**2-1** and **2-2**) appearing at t = 7.25 and 7.30 min are identified as 1,2-dimethylcyclohexa-1,4-diene and *trans*-5-methyl-1,3,6-heptatriene, respectively, by comparison with the National Institute of Standards and Technology/Wiley (NIST) standard library (Figure 2b,c). The C_4 residuals of the monomer are recognized in the structure of dimers as shown in Figure 2a (marked in red). Obviously, their formation is unintelligible on the basis of the addition polymerization of the triple bond in the alkynyl, which would produce a C−C═C(−C)−C(−C)═C−C skeleton but would be very easy if 1,3-butadiene is taken into account. **2-1** can result from the Diels−Alder reaction between 2-butyne and 1,3-butadiene, and **2-2** can result from an addition reaction between two 1,3-butadiene molecules (Figure 2a). The trimer appearing at t = 16.02 min (**3-3**) is recognized as 2,3-dimethyl-1,4,4a,5,8,8a-hexahydronaphthalene by examining the NIST database (Figure S6), likely resulting from the Diels−Alder reaction between **2-1** and another 1,3-butadiene. Its mass spectrum has a strong molecular ion peak, significantly different from those of other trimers (Figure S7). All of the other trimers and tetramers and the pentamer show very weak molecular ion peaks, suggesting that they are linear or branched molecules without extended conjugation (Figure 2d,e and Figure S7). This also excludes the direct addition polymerization of C≡C bonds which would produce conjugated C═C bonds, hence suggesting that the methyl groups are involved in the polymerization. Considering the $-CH_2-/R_3CH$ group identified in the spectroscopic result, it is most likely that methyl donated its hydrogen to the alkynyl, that is, intramolecular or intermolecular H-transfer under high pressure.

To investigate the H-transfer pathway, we studied the crystal structures of 2-butyne under high pressure. The lattice parameters of phases I and II at 1.2 and 1.8 GPa were determined by single-crystal X-ray diffraction (XRD, Table S3). The in situ synchrotron powder XRD shows that phase II is stable below 14.6 GPa (Figure S8a). Above that, the XRD peaks start to broaden and become indistinguishable, indicating the onset of amorphization/reaction, consistent with the Raman results. Hence, the crystal structure of 2-butyne under 12.2 GPa was investigated by Rietveld refinement as the critical structure (Figure S8c, Table S4), and the atomic positions were optimized by density functional theory (DFT) calculations in the Vienna Ab Initio Simulation Package (VASP) with the lattice parameters fixed to the experimental data. The linear 2-butyne molecules are stacked parallel with an inclined angle of 42° with respect to the c axis. The closest intermolecular distance between hydrogen in methyl group and carbon in alkynyl group (H···C_{sp}) is inside the layer and compressed to 2.08 Å (d_1 in Figure 3a) at 12.2

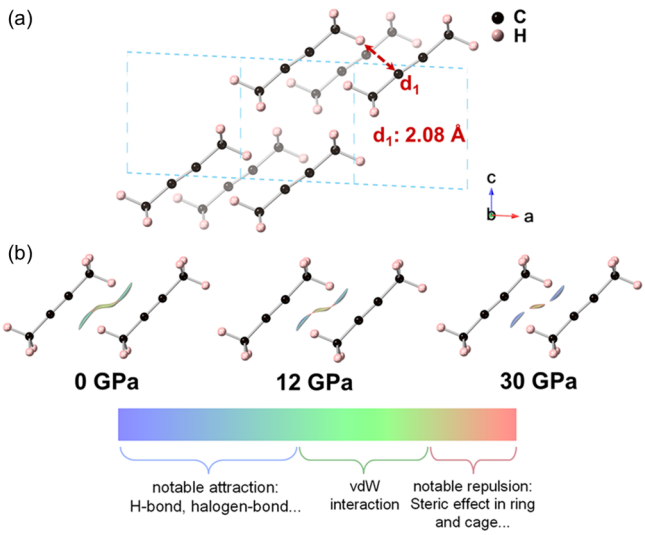

Figure 3. (a) Crystal structure of 2-butyne optimized by density functional theory (DFT) calculations based on the experimental lattice under 12.2 GPa (view along the b direction). (b) Intereaction region indicator (IRI) study of chemical bonds and weak intereactions. The blue part stands for notable attraction, the green part stands for weak interaction, and the red part stands for the repulsion between molecules.[29] The IRI isovalue is 1.1.

GPa, which is shorter than the sum of the van der Waals (vdW) radii of carbon and hydrogen (2.9 Å) by 0.82 Å (28%). This indicates the presence of a very strong intermolecular CH···π interaction,[8,27,28] and is confirmed by the theoretical calculation of the interaction region indicator (IRI).[29] As shown in Figure 3b, with increasing pressure, the intermolecular interaction changes from a vdW interaction to notable

https://doi.org/10.1021/acs.jpclett.2c00877
J. Phys. Chem. Lett. 2022, 13, 4170−4175

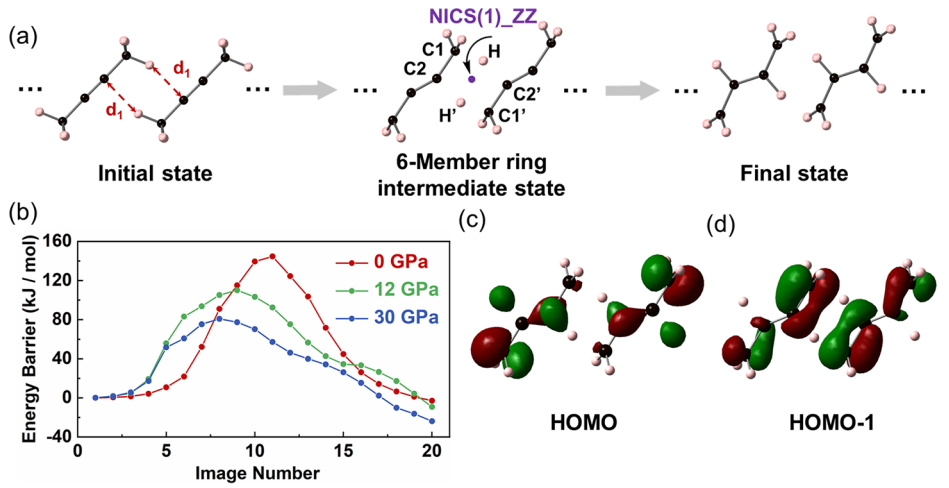

Figure 4. (a) H-transfer process of 2-butyne along d_1 in the NEB calculation. (b) Energy barrier vs image number of H-transfer under 0, 12, and 30 GPa. (c) HOMO and (d) HOMO − 1 of a six-membered ring intermediate state of H-transfer under 30 GPa.

attraction (at the CH···π) and repulsion (at the center of the six-membered ring), which indicates the possible H-transfer route.[8]

A theoretical investigation of the reaction mechanism was carried out in VASP at 0, 12, and 30 GPa. With the nudged elastic band (NEB) calculation, we found a concerted double-H transfer approximately along the intermolecular CH···π interaction based on the initial state of the 2-butyne crystal; that is, C1 donated a hydrogen to C2′ of the adjacent molecule, and C2 accepted a hydrogen from C1′ of the same neighbor simultaneously, going through a six-membered ring intermediate state (6-MRIS, a snapshot of the reaction process), −C2−C1−H−C2′−C1′−H′− (Figure 4a). This concerted H-transfer produced 1,3-butadiene, which perfectly explained the formation of the oligomers observed in HRGC−MS. As shown in Figure 4b, the energy of the final state 1,3-butadiene is significantly lower than that of 2-butyne under high pressure, which shows that the H-transfer reaction is thermodynamically favorable. The energy barrier of this H-transfer reaction decreases with increasing pressure, dropping from about 150 kJ/mol at 0 GPa to 81 kJ/mol at 30 GPa, which is low enough for the reaction to proceed at room temperature.

We also calculated the nucleus-independent chemical shift (NICS) of 6-MRIS with the two H atoms at the midway point in the transition.[30,31] NICS(1)_ZZ (NICS projections onto the normal vector of the ring plane of the atom 1 Å above the mass center of the ring) are −15.69 ppm under 0 GPa, −23.77 ppm under 12 GPa, and −24.26 ppm under 30 GPa. In contrast, the NICS(0)_ZZ values outside the six-membered ring are always positive (Figure S9 and Table S5). This indicates that the transition state of the H-transfer is aromatic and that the aromaticity is enhanced under external pressure. This is why such a transition becomes feasible.

The aromaticity can also be deduced from the perspective of frontier orbitals. We calculated the molecular orbitals with the relative positions of the molecular clusters fixed as in the crystal using Gaussian. The distributions of the highest occupied molecular orbital (HOMO) and HOMO − 1 (the first orbital below HOMO) of 6-MRIS at 30 GPa are shown in Figure 4c,d. HOMO has little to do with the discussed state and is not considered. The HOMO − 1 on the six-membered ring has two nodes, indicating that it is a Hückel system. Six electrons, including two π electrons (one from each molecule on average) and four σ electrons from the two C−H σ bonds, participated in this transfer process and satisfied the $4n + 2$ rule for an aromatic transition state. In the literature, similar sigmatropic H-transfer was studied theoretically, such as the synchronous [σ2s + σ2s + π2s] suprafacial double H-transfer from ethane to ethylene, and our study recognized this reaction of hydrocarbons under high pressure for the first time.[32]

At ambient pressure, the isomerization of C_4H_6 species occurs under base-catalyzed and combustion conditions.[33−36] In combustion chemistry, isomerization as an important intermediate process has attracted much attention.[34−39] A series of pyrolysis experiments of C_4H_6 species implied that fast isomerization occurs prior to C−C bond cleavage.[37,38] These unimolecular and H-assisted isomerizations require high temperature to overcome the high energy barrier.[34,35,39] Here we found that, under high pressure, isomerization can also be realized via intermolecular H-transfer at room temperature.

In conclusion, the H-transfer from CH_3 to C≡C via the C−H···π route in solid 2-butyne under high-pressure and room-temperature conditions was confirmed by vibrational spectroscopy, HRGC−MS, in situ XRD, and a theoretical simulation. A concerted intermolecular two-in−two-out H-transfer path via an aromatic [$4n + 2$] Hückel transition state was concluded. The suitable molecular conformation and the short H···C_{sp} distance are the keys to inducing this double H-transfer reaction. Our studies highlight the fact that the inert methyl group can be activated by alkynyl under high pressure through the C−H···π route, providing novel insights for understanding the conversion of C−H compounds under extreme conditions.

■ ASSOCIATED CONTENT

Supporting Information

The Supporting Information is available free of charge at https://pubs.acs.org/doi/10.1021/acs.jpclett.2c00877.

Experimental procedures and calculation details; supplementary figures and tables, including the synthesis of sample PE-20 and in situ high-pressure Raman, IR, single-crystal XRD, synchrotron powder XRD, high-resolution GC−MS, and MALDI-TOF-MS experiments and DFT calculations (PDF)

https://doi.org/10.1021/acs.jpclett.2c00877
J. Phys. Chem. Lett. 2022, 13, 4170−4175

AUTHOR INFORMATION

Corresponding Author

Haiyan Zheng − *Center for High Pressure Science and Technology Advanced Research, Beijing 100094, P. R. China;* orcid.org/0000-0002-4727-5912; Email: zhenghy@hpstar.ac.cn

Authors

Peijie Zhang − *Center for High Pressure Science and Technology Advanced Research, Beijing 100094, P. R. China;* orcid.org/0000-0001-6355-5482

Xingyu Tang − *Center for High Pressure Science and Technology Advanced Research, Beijing 100094, P. R. China*

Chunfang Zhang − *College of Chemistry and Environmental Science, Hebei University, Baoding 071002, P. R. China;* orcid.org/0000-0003-0768-0531

Dexiang Gao − *Center for High Pressure Science and Technology Advanced Research, Beijing 100094, P. R. China*

Xuan Wang − *Center for High Pressure Science and Technology Advanced Research, Beijing 100094, P. R. China;* orcid.org/0000-0001-6647-9542

Yajie Wang − *Center for High Pressure Science and Technology Advanced Research, Beijing 100094, P. R. China*

Wenhan Guo − *Great Bay University, Dongguan 523000, P. R. China*

Ruqiang Zou − *School of Materials Science and Engineering, Peking University, Beijing 100871, P. R. China;* orcid.org/0000-0003-0456-4615

Yehua Han − *State Key Laboratory of Heavy Oil Processing, College of Chemical Engineering and Environment, China University of Petroleum—Beijing, Beijing 102249, P. R. China;* orcid.org/0000-0002-8416-9860

Xiaohuan Lin − *Center for High Pressure Science and Technology Advanced Research, Beijing 100094, P. R. China*

Xiao Dong − *Key Laboratory of Weak-Light Nonlinear Photonics, School of Physics, Nankai University, Tianjin 300071, P. R. China*

Kuo Li − *Center for High Pressure Science and Technology Advanced Research, Beijing 100094, P. R. China;* orcid.org/0000-0002-4859-6099

Ho-kwang Mao − *Center for High Pressure Science and Technology Advanced Research, Beijing 100094, P. R. China*

Complete contact information is available at: https://pubs.acs.org/10.1021/acs.jpclett.2c00877

Author Contributions

$^{\nabla}$P.Z. and X.T. contributed equally.

Notes

The authors declare no competing financial interest.

ACKNOWLEDGMENTS

This study is funded by the National Key Research and Development Program of China (2019YFA0708502). The authors acknowledge the support of the National Natural Science Foundation of China (NSFC) (grant nos. 21875006, 22022101, and 21771011). This research used the resources of the Advanced Light Source, which is a U.S. Department of Engery (DOE) Office of Science User Facility under contract no. DE-AC02-05CH11231. This research also used the resources of the Pohang Accelerator Laboratory, Beijing Synchrotron Radiation Facility, and Shanghai Synchrotron Radiation Facility. The calculations were performed on the Tianhe-2 supercomputer at the Chinese National Supercomputer Center in Guangzhou. The authors thank Dr. Hyun Hwi Lee for his help with the in situ XRD measurements performed on the 5A XRS-MS beamline at the Pohang Accelerator Laboratory (PAL).

REFERENCES

(1) Kolesnikov, A. Y.; Saul, J. M.; Kutcherov, V. G. Chemistry of hydrocarbons under extreme thermobaric conditions. *ChemistrySelect* **2017**, *2*, 1336−1352.

(2) Kolesnikov, A.; Kutcherov, V. G.; Goncharov, A. F. Methane-derived hydrocarbons produced under upper-mantle conditions. *Nature Geosci.* **2009**, *2*, 566−570.

(3) Serovaiskii, A.; Kutcherov, V. Formation of complex hydrocarbon systems from methane at the upper mantle thermobaric conditions. *Sci. Rep.* **2020**, *10*, 4559.

(4) Snider, E.; Dasenbrock-Gammon, N.; McBride, R.; Debessai, M.; Vindana, H.; Vencatasamy, K.; Lawler, K. V.; Salamat, A.; Dias, R. P. Room-temperature superconductivity in a carbonaceous sulfur hydride. *Nature* **2020**, *586*, 373−377.

(5) Meier, T.; Petitgirard, S.; Khandarkhaeva, S.; Dubrovinsky, L. Observation of nuclear quantum effects and hydrogen bond symmetrisation in high pressure ice. *Nat. Commun.* **2018**, *9*, 2766.

(6) Guthrie, M.; Boehler, R.; Tulk, C. A.; Molaison, J. J.; dos Santos, A. M.; Li, K.; Hemley, R. J. Neutron diffraction observations of interstitial protons in dense ice. *Proc. Natl. Acad. Sci. U.S.A.* **2013**, *110*, 10552−10556.

(7) Pickard, C. J.; Needs, R. J. Highly compressed ammonia forms an ionic crystal. *Nat. Mater.* **2008**, *7*, 775−779.

(8) Zheng, H.; Li, K.; Cody, G. D.; Tulk, C. A.; Dong, X.; Gao, G.; Molaison, J. J.; Liu, Z.; Feygenson, M.; Yang, W.; Ivanov, I. N.; Basile, L.; Idrobo, J. C.; Guthrie, M.; Mao, H.-k. Polymerization of acetonitrile via a hydrogen transfer reaction from CH_3 to CN under extreme conditions. *Angew. Chem., Int. Ed.* **2016**, *55*, 12040−12044.

(9) Zhuravlev, K. K.; Traikov, K.; Dong, Z.; Xie, S.; Song, Y.; Liu, Z. Raman and infrared spectroscopy of pyridine under high pressure. *Phys. Rev. B* **2010**, *82*, 064116.

(10) Fanetti, S.; Citroni, M.; Bini, R. Structure and reactivity of pyridine crystal under pressure. *J. Chem. Phys.* **2011**, *134*, 204504.

(11) Fanetti, S.; Santoro, M.; Alabarse, F.; Enrico, B.; Bini, R. Modulating the H-bond strength by varying the temperature for the high pressure synthesis of nitrogen rich carbon nanothreads. *Nanoscale* **2020**, *12*, 5233−5242.

(12) Li, X.; Wang, T.; Duan, P.; Baldini, M.; Huang, H.-T.; Chen, B.; Juhl, S. J.; Koeplinger, D.; Crespi, V. H.; Schmidt-Rohr, K.; Hoffmann, R.; Alem, N.; Guthrie, M.; Zhang, X.; Badding, J. V. Carbon nitride nanothread crystals derived from pyridine. *J. Am. Chem. Soc.* **2018**, *140*, 4969−4972.

(13) Hay, S.; Pudney, C. R.; McGrory, T. A.; Pang, J.; Sutcliffe, M. J.; Scrutton, N. S. Barrier compression enhances an enzymatic hydrogen-transfer reaction. *Angew. Chem., Int. Ed.* **2009**, *48*, 1452−1454.

(14) Nishio, M.; Umezawa, Y.; Fantini, J.; Weissd, M. S.; Chakrabarti, P. CH−π hydrogen bonds in biological macromolecules. *Phys. Chem. Chem. Phys.* **2014**, *16*, 12648−12683.

(15) Nishio, M. The CH/π hydrogen bond: Implication in chemistry. *J. Mol. Struct.* **2012**, *1018*, 2−7.

(16) Steiner, T.; Koellner, G. Hydrogen bonds with π-acceptors in proteins: frequencies and role in stabilizing local 3D structures. *J. Mol. Biol.* **2001**, *305*, 535−557.

(17) Ozawa, T.; Okazaki, K.; Kitaura, K. Importance of CH/π hydrogen bonds in recognition of the core motif in proline-recognition domains: An Ab initio fragment molecular orbital study. *J. Comput. Chem.* **2011**, *32*, 2774−2782.

(18) Katrusiak, A.; Podsiadzo, M.; Budzianowski, A. Association CH···π and no Van der Waals contacts at the lowest limits of crystalline benzene I and II stability regions. *Cryst. Growth Des.* **2010**, *10*, 3461−3465.

(19) Sun, J.; Dong, X.; Wang, Y.; Li, K.; Zheng, H.; Wang, L.; Cody, G. D.; Tulk, C. A.; Molaison, J. J.; Lin, X.; Meng, Y.; Jin, C.; Mao, H.-k. Pressure-induced polymerization of acetylene: structure-directed stereoselectivity and a possible route to graphene. *Angew. Chem., Int. Ed.* **2017**, *56*, 6553−6557.
(20) Han, J.; Tang, X.; Wang, Y.; Wang, Y.; Han, Y.; Lin, X.; Dong, X.; Lee, H. H.; Zheng, H.; Li, K.; Mao, H.-k. Pressure-induced polymerization of monosodium acetylide: a radical reaction initiated topochemically. *J. Phys. Chem. C* **2019**, *123*, 30746−30753.
(21) Pasynkiewicz, S.; Oledzka, E.; Pietrzykowski, A. Polymerization of alkynes on nickelocene based catalysts: considerations on polymerization mechanism. *J. Mol. Catal. A: Chem.* **2004**, *224*, 117−124.
(22) Busico, V.; Cipullo, R.; Pellecchia, R.; Ronca, S.; Roviello, G.; Talarico, G. Design of stereoselective Ziegler-Natta propene polymerization catalysts. *Proc. Natl. Acad. Sci. U.S.A.* **2006**, *103*, 15321−15326.
(23) Kolesnikov, A. Y.; Saul, J. M.; Kutcherov, V. G. Chemistry of hydrocarbons under extreme thermobaric conditions. *ChemistrySelect* **2017**, *2*, 1336−1352.
(24) Baonza, V. G.; Montoro, O. R.; Taravillo, M.; Cáceres, M.; Núñez, J. Phase transitions and hindered rotation in dimethylacetylene at high pressures probed by Raman spectroscopy. *J. Chem. Phys.* **2004**, *121*, 11156−11162.
(25) Guan, J.; Daljeet, R.; Kieran, A.; Song, Y. Pressure-induced amorphization and reactivity of solid dimethyl acetylene probed by in situ FTIR and Raman spectroscopy. *J. Phys.: Condes. Matter* **2018**, *30*, 224004.
(26) Colthup, N. B.; Daly, L. H.; Wiberley, S. E. *Introduction to Infrared and Raman Spectroscopy*, 3rd ed., Academic Press, Inc., 1990.
(27) Nishio, M. The CH/π hydrogen bond in chemistry. Conformation, supramolecules, optical resolution and interactions involving carbohydrates. *Phys. Chem. Chem. Phys.* **2011**, *13*, 13873−13900.
(28) Holme, A.; Sæthre, L. J.; Bφrve, K. J.; Thomas, T. D. Carbon 1s photoelectron spectroscopy of 1-pentyne conformers. *J. Mol. Struct.* **2009**, *920*, 387−392.
(29) Lu, T.; Chen, Q. Interaction region indicator: a simple real space function clearly revealing both chemical bonds and weak interactions. *Chemistry-Methods* **2021**, *1*, 231−239.
(30) Schleyer, P. v. R.; Maerker, C.; Dransfeld, A.; Jiao, H.; van Eikema Hommes, N. J. R. Nucleus-independent chemical shifts: a simple and efficient aromaticity probe. *J. Am. Chem. Soc.* **1996**, *118*, 6317−6318.
(31) Chen, Z.; Wannere, C. S.; Corminboeuf, C.; Puchta, R.; Schleyer, P. v. R. Nucleus-independent chemical shifts (NICS) as an aromaticity criterion. *Chem. Rev.* **2005**, *105*, 3842−3888.
(32) Schleyer, P. v. R.; Wu, J. I.; Cossío, F. P.; Fernández, I. Aromaticity in transition structures. *Chem. Soc. Rev.* **2014**, *43*, 4909−4921.
(33) Calihan, L. E.; Kay, E. L.; Roberts, D. T., Jr; Wakefield, L. B. Synthesis of 1,2-butadiene. Vapor phase isomerization of 2-butyne over base-modified catalysts. *Ind. Eng. Chem. Prod. Res. Dev.* **1975**, *14*, 287−290.
(34) Huang, C.; Yang, B.; Zhang, F. Initiation mechanism of 1,3-butadiene combustion and its effect on soot precursors. *Combust. Flame* **2017**, *184*, 167−175.
(35) Pham, T. V.; Tue Trang, H. T. Theoretical investigation of the mechanisms and kinetics of the bimolecular and unimolecular reactions involving in the C_4H_6 species. *J. Phys. Chem. A* **2021**, *125*, 585−596.
(36) Lockhart, J. P. A.; Goldsmith, C. F.; Randazzo, J. B.; Ruscic, B.; Tranter, R. S. An experimental and theoretical study of the thermal decomposition of C_4H_6 isomers. *J. Phys. Chem. A* **2017**, *121*, 3827−3850.
(37) Hidaka, Y.; Higashihara, T.; Ninomiya, N.; Masaoka, H.; Nakamura, T.; Kawano, H. Shock tube and modeling study of 1, 3-butadiene pyrolysis. *Int. J. Chem. Kinet.* **1996**, *28*, 137−151.
(38) Chambreau, S. D.; Lemieux, J.; Wang, L.; Zhang, J. Mechanistic studies of the pyrolysis of 1,3-butadiene, 1,3-butadiene-1,1,4,4-d_4, 1,2-butadiene, and 2-butyne by supersonic jet/photoionization mass spectrometry. *J. Phys. Chem. A* **2005**, *109*, 2190−2196.
(39) Hidaka, Y.; Higashihara, T.; Ninomiya, N.; Oshita, H.; Kawano, H. Thermal isomerization and decomposition of 2-butyne in shock waves. *J. Phys. Chem.* **1993**, *97*, 10977−10983.

https://doi.org/10.1021/acs.jpclett.2c00877
J. Phys. Chem. Lett. 2022, 13, 4170−4175